MODEL-BASED ITERATIVE RECONSTRUCTION ENABLES THE EVALUATION OF THIN-SLICE COMPUTED TOMOGRAPHY IMAGES WITHOUT DEGRADING IMAGE QUALITY OR INCREASING RADIATION DOSE.

Aurumskjöld, Marie-Louise; Ydström, Kristina; Tingberg, Anders; Söderberg, Marcus

Published in:
Radiation Protection Dosimetry

DOI:
10.1093/rpd/ncv474

Published: 2016-06-01

Document Version
Peer reviewed version (aka post-print)

MODEL-BASED ITERATIVE RECONSTRUCTION ENABLES THE EVALUATION OF THIN SLICE COMPUTED TOMOGRAPHY IMAGES WITHOUT DEGRADING IMAGE QUALITY OR INCREASING RADIATION DOSE

Authors: Marie-Louise Aurumskjöld[1], Kristina Ydström[2], Anders Tingberg[1], Marcus Söderberg[1]

Address: [1]Medical Radiation Physics Malmö, Department of Translational Medicine, Lund University, Skåne University Hospital, SE-205 02 Malmö, Sweden

[2] Philips Healthcare, SE-211 24 Malmö, Sweden

Corresponding author: Marie-Louise Aurumskjöld

Telephone: +46 46 17 31 35

Fax: +46 40 96 31 85

E-mail: marie.louise.aurumskjold@med.lu.se

Short running title: Model-based iterative reconstruction

MODEL-BASED ITERATIVE RECONSTRUCTION ENABLES THE EVALUATION OF THIN SLICE COMPUTED TOMOGRAPHY IMAGES WITHOUT DEGRADING IMAGE QUALITY OR INCREASING RADIATION DOSE

Marie-Louise Aurumskjöld, Kristina Ydström, Anders Tingberg, Marcus Söderberg

ABSTRACT

Computed tomography (CT) is one of the most important modalities in a radiological department. This technique produces images that enables radiological reports with high diagnostic confidence, but may provide an elevated radiation dose to the patient. The radiation dose can be reduced by using advanced image reconstruction algorithms. This study was performed on a Brilliance iCT, equipped with iDose^4 iterative reconstruction and an iterative model-based reconstruction (IMR) method. The purpose was to investigate the effect of reduced slice thickness combined with an IMR method on image quality compared with standard slice thickness with iDose^4 reconstruction. The results of objective and subjective image quality evaluations showed that a thinner slice combined with IMR can improve the image quality and reduce partial volume artefacts compared with the standard slice thickness with iDose^4. In conclusion, IMR enables reduction of the slice thickness while maintaining or even improving image quality versus iDose^4.

INTRODUCTION

Computed tomography (CT) examinations constitute about 50-60% of the collective effective radiation dose, but represent only about 15% of the total number of radiological examinations[(1)]. The number of CT examinations performed is continuously increasing; therefore, it is important to find methods to lower the radiation dose and establish sufficient image quality for a specific diagnostic task. One such method is to use advanced algorithms for image reconstruction[(2)]. There is constant development of new reconstruction methods to gain better image quality or to reduce the radiation dose[(3)]. The conventional filtered back-projection (FBP) procedure is being replaced by iterative reconstruction methods. Several clinical studies have shown the potential of iterative reconstruction to improve image quality while reducing the radiation dose[(4-6)]. The purpose of this study was to investigate the effect on image quality of reduced slice thickness combined with a model-based iterative reconstruction (IMR) method compared with standard slice thickness (5 mm) with iDose^4 reconstruction.

MATERIALS AND METHODS

Equipment

The study was performed on a Brilliance iCT (Philips Healthcare, Cleveland, OH, USA), with FBP and two different iterative reconstruction methods, iDose^4 and IMR (prototype v. 1.2.0.0 R07). Optimization of iDose^4, a hybrid iterative reconstruction, is based on photon statistics, assuming an ideal system. The IMR optimization also attempts to model the system and the acquisition process, including system optics. Both reconstructions utilize data in the projection domain. To evaluate the effect of slice thickness on image quality, an image quality phantom (Catphan® 600, The Phantom Laboratory Inc, Greenwich, NY, USA) and an anthropomorphic phantom (CTU-41, Kyoto Kagaku, Kyoto, Japan) were used.

Catphan® – noise and subjective low-contrast resolution

The Catphan® phantom was scanned at a fixed CT dose index volume ($CTDI_{vol}$). Images were reconstructed with FBP as well as different levels of $iDose^4$ and IMR. All parameters are shown in Table 1. Images were reconstructed with different slice thicknesses (1, 3, and 5 mm). Image noise (one standard deviation [SD] of the CT-numbers) was measured in the homogeneous module of Catphan® (Figure 1A). Low-contrast resolution was subjectively assessed using the low-contrast module of the phantom. The module contains three sets of outer supra-slice cylinders (Figure 1B). The three cylinder sets have a nominal contrast of 1.0% (~10 Hounsfield units, HU), 0.5% (~5 HU), and 0.3% (~3 HU) to the background and each set consists of nine cylinders with diameters ranging from 2 to 15 mm[(7)]. Subjective assessment of all reconstructions was carried out in consensus by three observers. Visibility of the three sets of supra-slice cylinders was determined as the smallest discernible cylinder and the smallest sharply defined cylinder. The images were presented individually using the viewing and scoring software ViewDEX v. 2.0[(8)] and shown in randomized order on a picture archiving and communication system (PACS) workstation. The window level was adjusted for each reconstruction to match the mean attenuation in the homogeneous background, while window width was fixed at 80 HU.

Anthropomorphic phantom – contrast-to-noise ratio in the liver

The anthropomorphic phantom was scanned at a fixed $CTDI_{vol}$. The dose level was chosen according to a routine clinical protocol. Images of different slice thicknesses (1, 3, and 5 mm) were reconstructed using FBP and different levels of $iDose^4$ and IMR. All scanning and reconstruction parameters are shown in Table 1. One slice of the anthropomorphic phantom, covering both the liver and one kidney, was used for measuring the CT numbers (HU) and

noise using identical regions of interest (ROIs) placed in the liver and background, (Figure 1C). Contrast-to-noise ratios (CNRs) were calculated using equation (1):

$$CNR = \frac{HU_{Liver} - HU_{Background}}{SD} \qquad (1)$$

Clinical case – noise in the liver

Raw data from one patient referred for routine abdominal CT was used to reconstruct images of different slice thicknesses (1, 3, and 5 mm) and levels of iDose^4 and IMR. Level 2 iDose^4 is routinely used in the clinic. Measurements of the CT number and the noise were made in a homogeneous region of the liver.

RESULTS

Catphan® – noise and subjective low-contrast resolution

An objective evaluation of image noise in the homogeneous module of Catphan® showed that a thinner slice with IMR provided less noise than a thicker slice with iDose4. The results of the objective evaluation are shown in Figure 2. The noise reduction when using thicker slices with IMR was small, and the effect was even smaller for higher levels of IMR. Example images of the low-contrast resolution module reconstructed with different algorithms and slice thicknesses are shown in Figure 3. The visibility of low-contrast objects for the thinnest slices with IMR reconstructed images was higher than the thickest slices reconstructed with iDose^4 and FBP. The results of the subjective assessment (discernible cylinders) are shown in Figure 4. The highest level of iDose^4 (L5) with a 5 mm slice thickness produced the same result as IMR at the lowest level (L1) with a 1 mm slice thickness. The number of discernible cylinders at the contrast level of 1.0% was almost the same for different slice thicknesses and IMR reconstruction levels, and IMR had the highest number of discernible cylinders at all three

contrast levels. No sharply defined cylinders were seen using FBP and iDose^4. The number of sharply defined cylinders at a contrast level of 1.0% was in the range of 1-2 with IMR.

Anthropomorphic phantom – contrast-to-noise ratio in the liver

The CNRs measured in the liver of the anthropomorphic phantom are shown in Figure 5. As expected, the CNR increased with increasing slice thickness and increasing levels of iDose^4 and IMR. The lowest CNR was found with FBP and a 1 mm slice thickness.

Clinical case – noise in the liver

An example of a routine abdominal CT examination, reconstructed with different levels of iDose4 and IMR for different slice thicknesses, is shown in Figure 6. This clinical case showed similar results as for the phantom measurements. Image noise measured in the liver for different slice thicknesses is shown in Figure 7. The results showed that IMR was only to a small degree dependent on slice thickness, contrary to iDose^4, and this effect was even smaller for higher levels of IMR.

DISCUSSION

Many studies have shown that there is a great potential to lower the radiation dose with iterative reconstruction methods[9-12]. In this study we investigated the impact of using thinner slices with the IMR algorithm, using two different phantoms and a clinical case. Results from the phantom study showed that it was possible to use a thinner slice with IMR compared with conventional iterative reconstruction with iDose^4, giving a better resolution in the z-direction. This was due to the strong noise reduction and enhanced low-contrast with IMR.

The low-contrast resolution is an important parameter to study since it may be critical, e.g., in brain and liver examinations. Low-contrast detectability is vital to the diagnostic

accuracy and normally high doses are required to achieve a good low-contrast resolution. With iterative reconstruction methods, it was possible to lower the noise and improve the low-contrast. Image noise was quantified by the SD of the HU-values measured in a ROI. This assumes that the noise distribution does not differ between FBP and iterative reconstruction. This may limit the use of objective image quality parameters and shows the importance of a subjective evaluation. The subjective assessment showed that the highest low-contrast resolution was obtained with IMR and was almost independent of slice thickness. Information about noise characteristics can be obtained by calculating the noise power spectrum (NPS). The NPS gives information about the noise texture in images and is ideal for detecting changes in noise distribution between different reconstructions. The shape of the NPS curves is similar between FBP and iDose^4, but considerably different for IMR[13]. Some radiologists claim that images reconstructed with iterative reconstruction methods have an unnatural appearance, and the different NPS curves may be the explanation for this.

By studying a clinical case, we verified the results from the phantom studies. Images of the clinical case were not reconstructed using FBP since the acquisition parameters include iDose^4 at level 2 and the radiation dose is optimized to this level. The effective noise reduction of IMR makes it possible to use 1 mm thin slices compared to 5 mm with iDose^4. The selection of slice thickness is usually a balance with noise as they work against each other, but with IMR, thinner slices can be used without compromising image quality. With a thinner slice, the effect of partial volume artefacts is also reduced.

Limitations of the study included that the phantom was only scanned once and the different reconstruction methods were applied to this scanned image set. This means that the uncertainty of the measures cannot be estimated based on the results. Variations between repeated scans with identical parameters in modern CT systems are very small; variations are caused by inconsistency in the signal chain. This inconsistency is not large enough to affect

the image quality parameters. Another limitation of this study is that only one clinical case was evaluated. The patient was of the same size as the anthropomorphic phantom to compare with the results obtained in phantom measurements. The results may not applicable among patients with a considerably different size and should be further investigated.

CONCLUSION

With IMR, it was possible to reduce the slice thickness while maintaining or even improving the image quality compared with what is achievable with iDose^4 and a thicker slice.

FUNDING

The authors would like to thank Region Skåne (Skane county council´s research and development foundation) for financial support.

TABLE LEGENDS

Table 1. Scan and reconstruction parameters.

Table 1.

Parameters	Catphan®	Anthropomorphic phantom
Tube voltage (kV)	120	120
Rotation time (s)	1	0.5
Collimation (mm)	128×0.625	128×0.625
Slice Thickness (mm)	1, 3, 5	1, 3, 5
Increment (mm)	1, 3, 5	1, 3, 5
Automatic exposure control	Off	ACS + Z-DOM
Pitch	0.601	0.933
Field of view (mm)	350	350
Filter	Standard B (FBP, iDose^4)	Standard B (FBP, iDose^4)
	Routine (IMR)	Routine (IMR)
Reconstruction algorithms	FBP, iDose^4 (L1, L3, L5)	FBP, iDose^4 (L1, L3, L5)
	IMR (L1, L2, L3)	IMR (L1, L2, L3)
$CTDI_{vol}$ (mGy)	10	7.1

FIGURE LEGENDS

Figure 1. Catphan® images for assessment of image noise (A) and low contrast resolution (B). The placement of the region of interest used for noise measurements is shown in (A). (C) An abdominal slice of the anthropomorphic phantom showing region of interest placements in the liver and the background used for determination of the contrast-to-noise ratio.

Figure 2. Image noise (one standard deviation [SD] of the CT number) measured in Catphan® for different slice thicknesses and reconstruction algorithms. FBP, filtered back-projection; ID, iDose^4; IMR, iterative model reconstruction; L, level.

Figure 3. Images of the low contrast module of Catphan® for different slice thicknesses and reconstruction algorithms. FBP, filtered back-projection; ID, iDose^4; IMR, iterative model reconstruction; L, level.

Figure 4. Subjective evaluation of low contrast resolution in Catphan®. A cumulative representation of the number of discernible cylinders at three contrast levels (0.3%, 0.5%, and 1.0%) for different slice thicknesses and reconstruction algorithms. Each bar shows the number of discernible objects at each contrast level, e.g. for FBP – 5 mm; 6 objects were discernible at 1.0% contrast, 3 at 0.5%, and none at 0.3%. FBP, filtered back-projection; ID, iDose^4; IMR, iterative model reconstruction; L, level.

Figure 5. Contrast-to-noise ratio measured in the liver of the anthropomorphic phantom for different slice thicknesses and reconstruction algorithms. FBP, filtered back-projection; ID, iDose^4; IMR, iterative model reconstruction; L, level.

Figure 6. A clinical case reconstructed with different slice thicknesses and reconstruction algorithms, showing the impact on image noise. ID, iDose^4; IMR, iterative model reconstruction, L, level.

Figure 7. Image noise measured in the liver for a clinical case for different slice thicknesses and reconstruction algorithms. ID, iDose^4; IMR, iterative model reconstruction, L, level.

Figure 1.

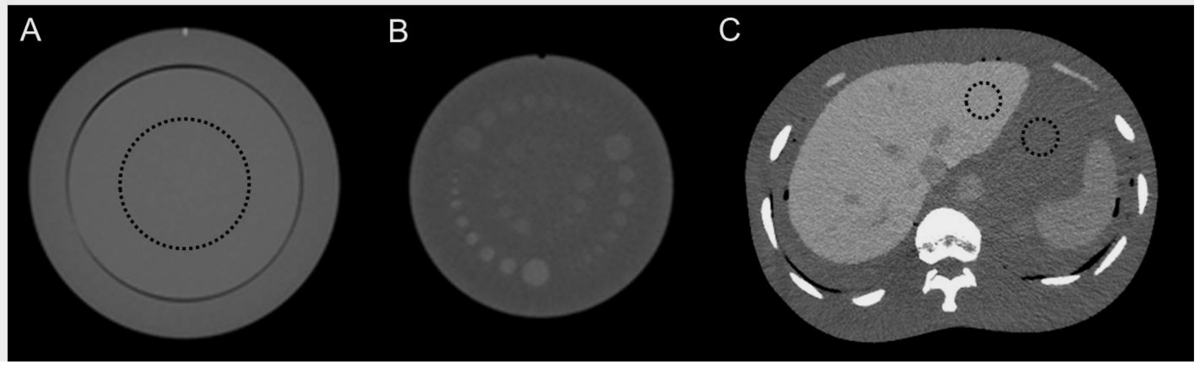

Figure 2.

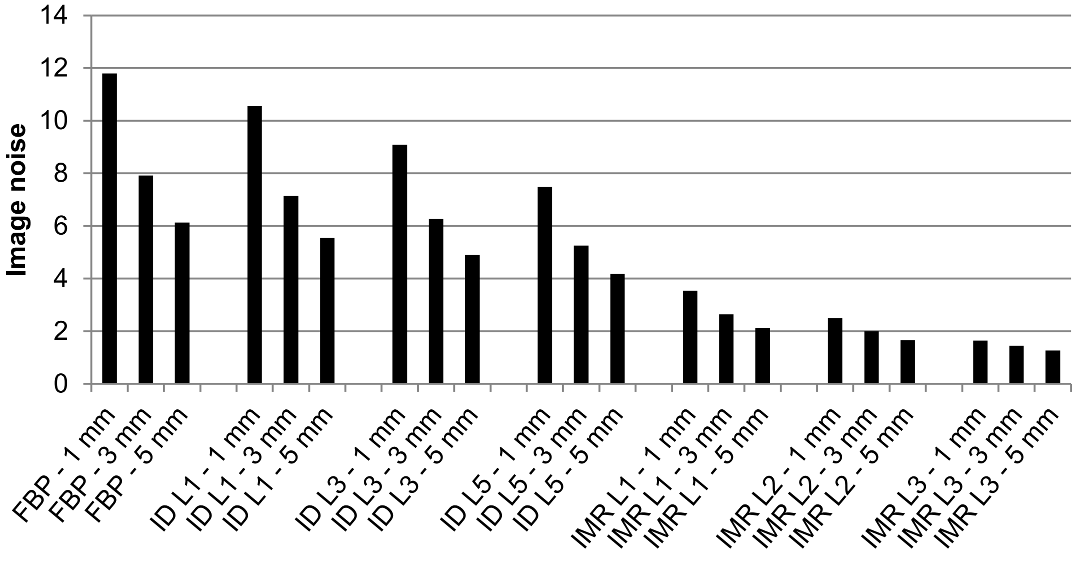

Image noise
14
12
10
8
6
4
2
0
FBP - 1 mm
FBP - 3 mm
FBP - 5 mm
ID L1 - 1 mm
ID L1 - 3 mm
ID L1 - 5 mm
ID L3 - 1 mm
ID L3 - 3 mm
ID L3 - 5 mm
ID L5 - 1 mm
ID L5 - 3 mm
ID L5 - 5 mm
IMR L1 - 1 mm
IMR L1 - 3 mm
IMR L1 - 5 mm
IMR L2 - 1 mm
IMR L2 - 3 mm
IMR L2 - 5 mm
IMR L3 - 1 mm
IMR L3 - 3 mm
IMR L3 - 5 mm

Figure 3.

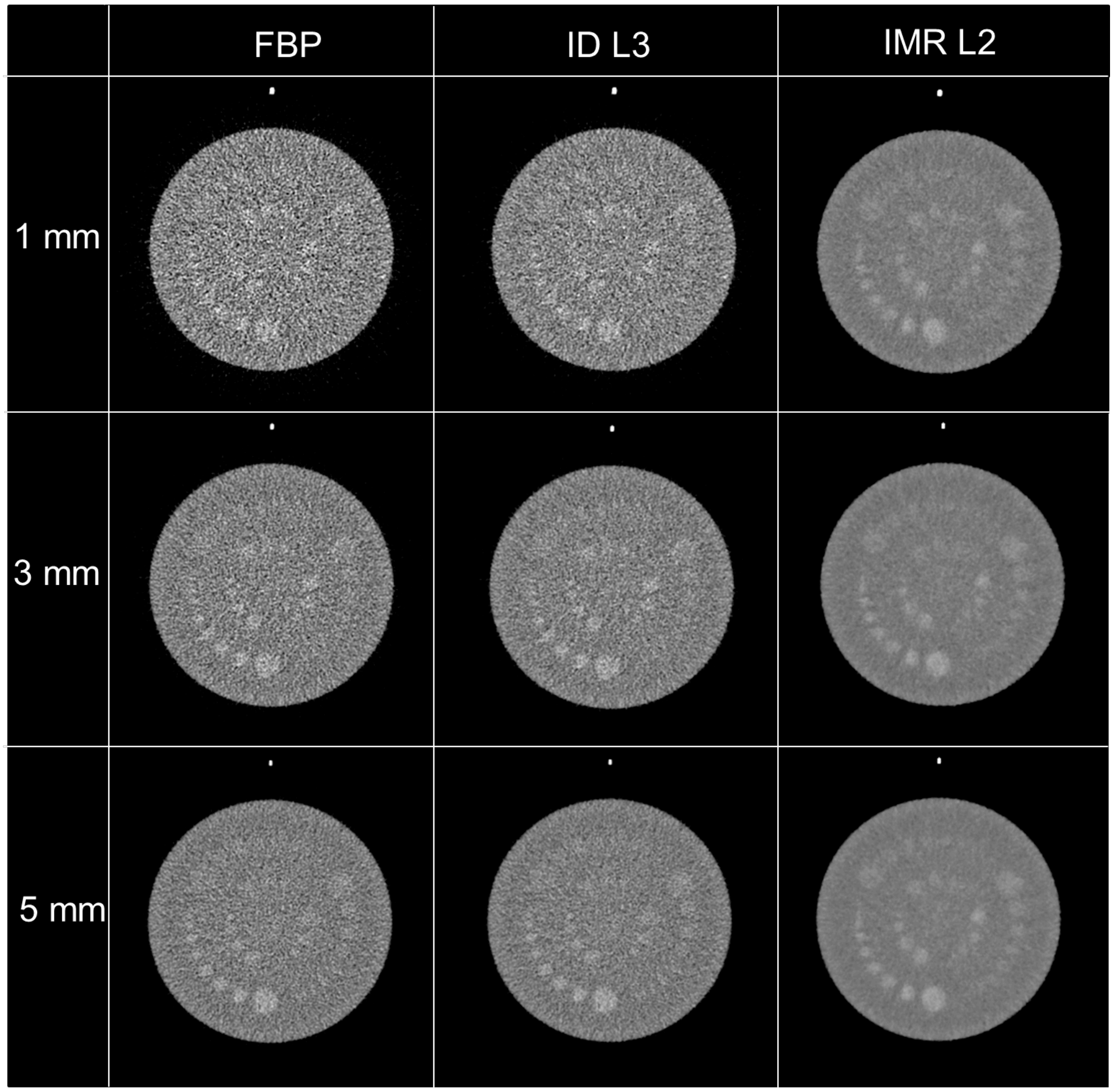

Figure 4.

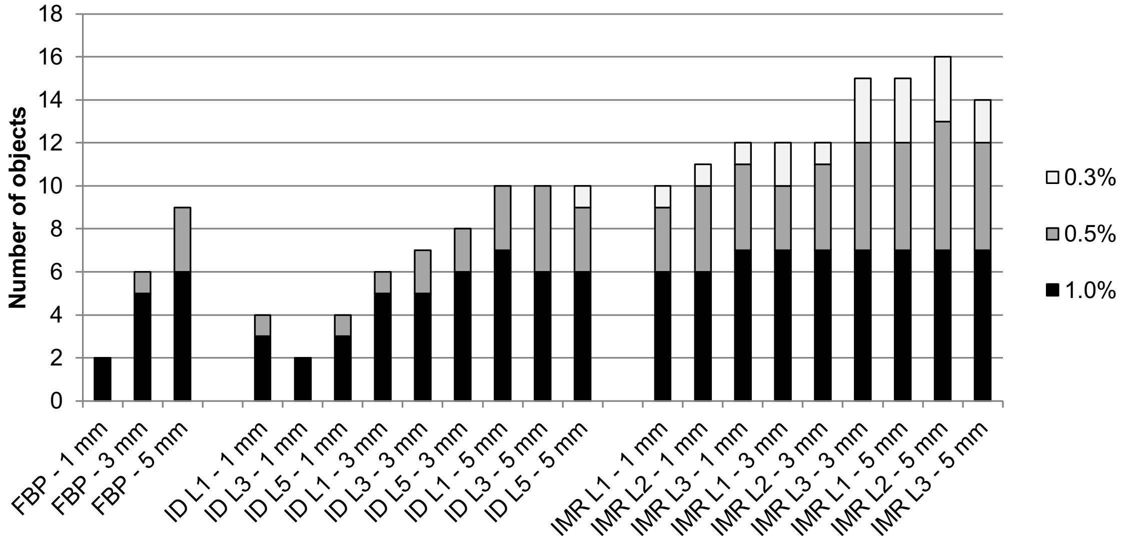

Number of objects
0
2
4
6
8
10
12
14
16
18
0.3%
0.5%
1.0%
FBP - 1 mm
FBP - 3 mm
FBP - 5 mm
ID L1 - 1 mm
ID L3 - 1 mm
ID L5 - 1 mm
ID L1 - 3 mm
ID L3 - 3 mm
ID L5 - 3 mm
ID L1 - 5 mm
ID L3 - 5 mm
ID L5 - 5 mm
IMR L1 - 1 mm
IMR L2 - 1 mm
IMR L3 - 1 mm
IMR L1 - 3 mm
IMR L2 - 3 mm
IMR L3 - 3 mm
IMR L1 - 5 mm
IMR L2 - 5 mm
IMR L3 - 5 mm

Figure 5.

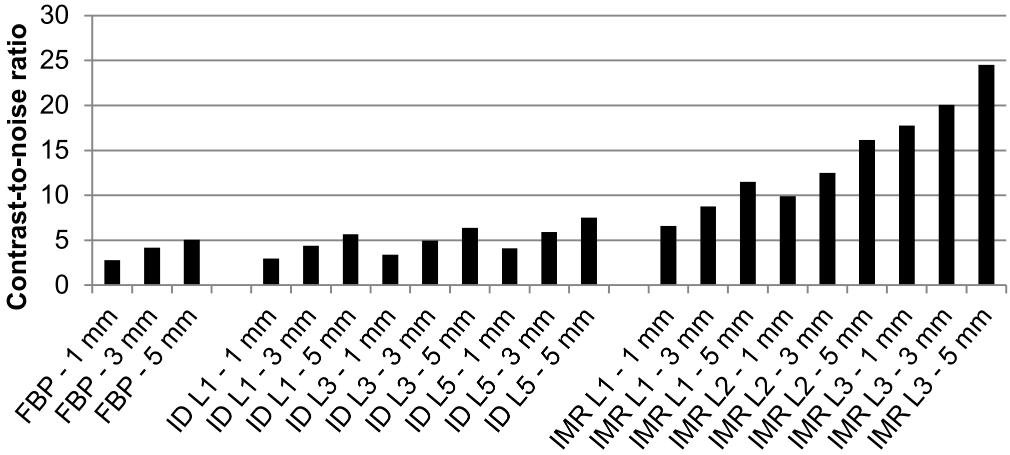
Contrast-to-noise ratio
30
25
20
15
10
5
0
FBP - 1 mm
FBP - 3 mm
FBP - 5 mm
ID L1 - 1 mm
ID L1 - 3 mm
ID L1 - 5 mm
ID L3 - 1 mm
ID L3 - 3 mm
ID L3 - 5 mm
ID L5 - 1 mm
ID L5 - 3 mm
ID L5 - 5 mm
IMR L1 - 1 mm
IMR L1 - 3 mm
IMR L1 - 5 mm
IMR L2 - 1 mm
IMR L2 - 3 mm
IMR L2 - 5 mm
IMR L3 - 1 mm
IMR L3 - 3 mm
IMR L3 - 5 mm

Figure 6.

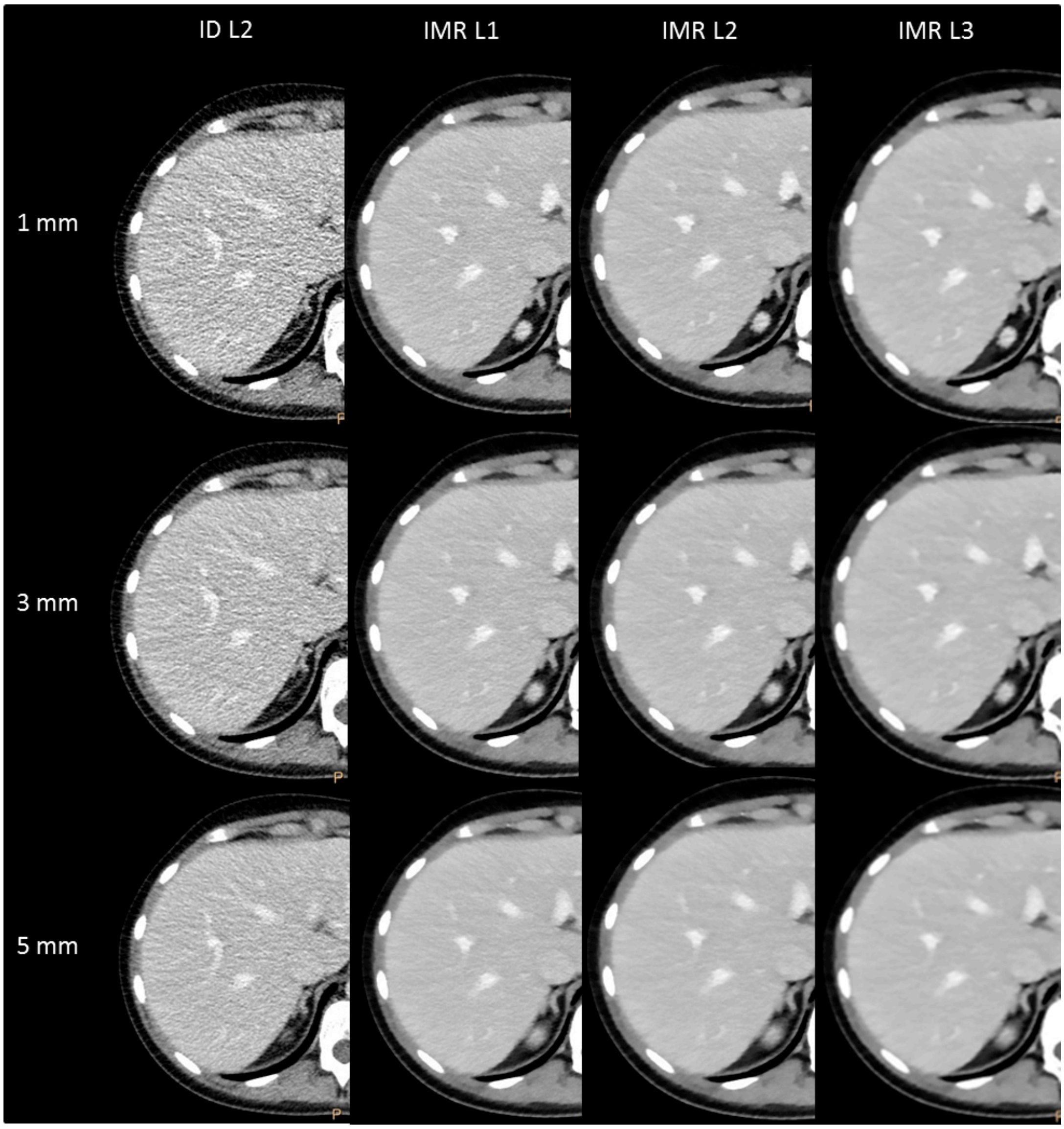

Figure 7.

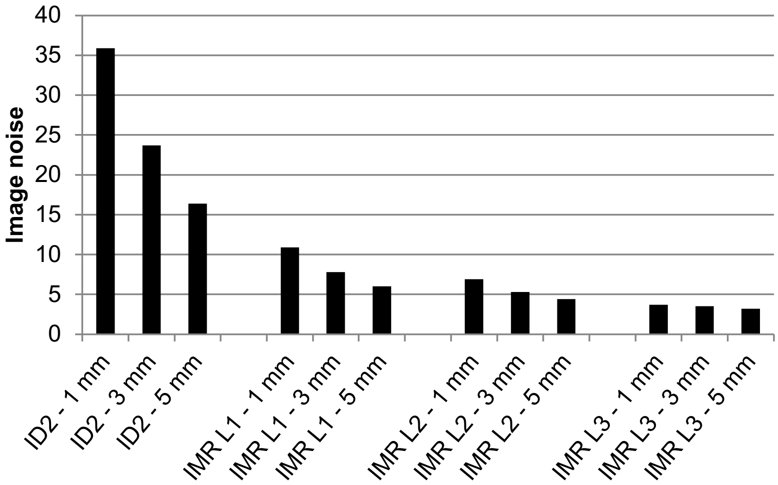

Image noise
40
35
30
25
20
15
10
5
0
ID2 - 1 mm
ID2 - 3 mm
ID2 - 5 mm
IMR L1 - 1 mm
IMR L1 - 3 mm
IMR L1 - 5 mm
IMR L2 - 1 mm
IMR L2 - 3 mm
IMR L2 - 5 mm
IMR L3 - 1 mm
IMR L3 - 3 mm
IMR L3 - 5 mm

REFERENCES

1. Almén, A., Richter, S. and Leitz, W. Swedish Radiation Protection. Authority report 2008:03: number of radiological examinations in Sweden (in Swedish) (2008).
2. Kalender, W.A., Buchenau, S.. Deak, P., Kellermeier, M., Langner, O., van Strafen, M., Vollmar, S. and Wilharm, S. Technical approaches to the optimisation of CT. Phys. Med. 24. 71-79 (2008).
3. Willemink, M.J., de Jong, P.A., Leiner, T., de Heer, L.M., Nievelstein, R.A., Budde, R.P. and Schilham, A.M. Iterative reconstruction techniques for computed tomography Part 1: Technical principles. Eur. Radiol. 23, 1623-1631 (2013).
4. Pontana, F.. Duhamel, A.. Pagniez, J.. Flohr, T.. Faivre, J.B., Hachulla, A.L., Remy, J. and Remy-Jardin, M. Chest computed tomography using iterative reconstruction vs filtered back projection (Part 2): image quality of low-dose CT examinations in 80 patients. Eur. Radiol. 21, 636-643 (2011).
5. Yamada, Y., Jinzaki, M., Hosokawa, T., Tanami, Y., Sugiura, H., Abe, T. and Kuribayashi, S. Dose reduction in chest CT: comparison of the adaptive iterative dose reduction 3D, adaptive iterative dose reduction, and filtered back projection reconstruction techniques. Eur. J. Radiol. 81, 4185-4195 (2012).
6. Deeder, R., Khawaja, A., Singh, S., Gilman, M., Sharma, A., Do, S., Pourjabbar, S., Padole, A., Lira, D., Brown, K., Shepard, J.A. and Kalra, M.K. Computed Tomography (CT) of the chest at less than 1 mSv: An ongoing prospective clinical trial of chest CT at submillisievert radiation doses with iterative model image reconstruction and iDose^4 technique. J. Comput. Assist. Tomogr. 38, 613-619 (2014).
7. The Phantom Laboratory. Catphan® 500 and 600 Manual. (2006).
8. Börjesson, S., Håkansson, M., Båth, M., Kheddache, S., Svensson, S., Tingberg, A., Grahn, A., Ruschin, M., Hemdal, B., Mattsson, S. and Månsson, L.G. . A software tool

for increased efficiency in observer performance studies in radiology. Radiat. Prot. Dosim. 114, 45-52 (2005).

9. Philips Electronics. $iDose^4$ iterative reconstruction technique. 1-40 (2011).

10. Mehta, D., Thompson, T., Morton, T., Dhanantwari, A. and Shefer, E. Iterative model reconstruction: simultaneously lowered computed tomography radiation dose and improved image quality. Med. Phys. Int. 1, 147-155 (2013).

11. Olsson, M-L. and Norrgren, K. An investigation of the iterative reconstruction method $iDose^4$ on a Philips CT Brilliance 64 using a Catphan 600 phantom. Proc. SPIE. 8313, doi 10.1117/12.910889 (2012).

12. Olsson, M-L., Norrgren, K. and Söderberg, M. Improvement of CT imaging quality with iterative reconstruction $iDose^4$. Conference paper ECR. dx.doi.org/10.1594/ecr2014/C-0387 (2014).

13. Löve, A., Olsson, M-L., Siemund, R., Stålhammar, F., Björkman-Burtscher, I.M. and Söderberg. M. Six iterative reconstruction algorithms in brain CT: a phantom study on image quality at different radiation dose levels. Br. J. Radiol. 86, 20130388 (2013).